

Search for Low-Mass Dark-Sector Higgs Bosons

J. P. Lees,¹ V. Poireau,¹ V. Tisserand,¹ J. Garra Tico,² E. Grauges,² D. A. Milanese,^{3a} A. Palano,^{3a,3b} M. Pappagallo,^{3a,3b} G. Eigen,⁴ B. Stugu,⁴ D. N. Brown,⁵ L. T. Kerth,⁵ Yu. G. Kolomensky,⁵ G. Lynch,⁵ H. Koch,⁶ T. Schroeder,⁶ D. J. Asgeirsson,⁷ C. Hearty,⁷ T. S. Mattison,⁷ J. A. McKenna,⁷ A. Khan,⁸ V. E. Blinov,⁹ A. R. Buzykaev,⁹ V. P. Druzhinin,⁹ V. B. Golubev,⁹ E. A. Kravchenko,⁹ A. P. Onuchin,⁹ S. I. Serednyakov,⁹ Yu. I. Skovpen,⁹ E. P. Solodov,⁹ K. Yu. Todyshev,⁹ A. N. Yushkov,⁹ M. Bondioli,¹⁰ D. Kirkby,¹⁰ A. J. Lankford,¹⁰ M. Mandelkern,¹⁰ H. Atmacan,¹¹ J. W. Gary,¹¹ F. Liu,¹¹ O. Long,¹¹ G. M. Vitug,¹¹ C. Campagnari,¹² T. M. Hong,¹² D. Kovalskyi,¹² J. D. Richman,¹² C. A. West,¹² A. M. Eisner,¹³ J. Kroseberg,¹³ W. S. Lockman,¹³ A. J. Martinez,¹³ T. Schalk,¹³ B. A. Schumm,¹³ A. Seiden,¹³ D. S. Chao,¹⁴ C. H. Cheng,¹⁴ D. A. Doll,¹⁴ B. Echenard,¹⁴ K. T. Flood,¹⁴ D. G. Hitlin,¹⁴ P. Ongmongkolkul,¹⁴ F. C. Porter,¹⁴ A. Y. Rakitin,¹⁴ R. Andreassen,¹⁵ Z. Huard,¹⁵ B. T. Meadows,¹⁵ M. D. Sokoloff,¹⁵ L. Sun,¹⁵ P. C. Bloom,¹⁶ W. T. Ford,¹⁶ A. Gaz,¹⁶ M. Nagel,¹⁶ U. Nauenberg,¹⁶ J. G. Smith,¹⁶ S. R. Wagner,¹⁶ R. Ayad,^{17,*} W. H. Toki,¹⁷ B. Spaan,¹⁸ M. J. Kobel,¹⁹ K. R. Schubert,¹⁹ R. Schwierz,¹⁹ D. Bernard,²⁰ M. Verderi,²⁰ P. J. Clark,²¹ S. Playfer,²¹ D. Bettoni,^{22a} C. Bozzi,^{22a} R. Calabrese,^{22a,22b} G. Cibinetto,^{22a,22b} E. Fioravanti,^{22a,22b} I. Garzia,^{22a,22b} E. Luppi,^{22a,22b} M. Munerato,^{22a,22b} M. Negrini,^{22a,22b} L. Piemontese,^{22a} V. Santoro,^{22a} R. Baldini-Ferroli,²³ A. Calcaterra,²³ R. de Sangro,²³ G. Finocchiaro,²³ P. Patteri,²³ I. M. Peruzzi,^{23,†} M. Piccolo,²³ M. Rama,²³ A. Zallo,²³ R. Contri,^{24a,24b} E. Guido,^{24a,24b} M. Lo Vetere,^{24a,24b} M. R. Monge,^{24a,24b} S. Passaggio,^{24a} C. Patrignani,^{24a,24b} E. Robutti,^{24a} B. Bhuyan,²⁵ V. Prasad,²⁵ C. L. Lee,²⁶ M. Morii,²⁶ A. J. Edwards,²⁷ A. Adametz,²⁸ J. Marks,²⁸ U. Uwer,²⁸ H. M. Lacker,²⁹ T. Lueck,²⁹ P. D. Dauncey,³⁰ P. K. Behera,³¹ U. Mallik,³¹ C. Chen,³² J. Cochran,³² W. T. Meyer,³² S. Prell,³² A. E. Rubin,³² A. V. Gritsan,³³ Z. J. Guo,³³ N. Arnaud,¹ M. Davier,¹ D. Derkach,¹ G. Grosdidier,¹ F. Le Diberder,¹ A. M. Lutz,¹ B. Malaescu,¹ P. Roudeau,¹ M. H. Schune,¹ A. Stocchi,¹ G. Wormser,¹ D. J. Lange,³⁵ D. M. Wright,³⁵ I. Bingham,³⁶ C. A. Chavez,³⁶ J. P. Coleman,³⁶ J. R. Fry,³⁶ E. Gabathuler,³⁶ D. E. Hutchcroft,³⁶ D. J. Payne,³⁶ C. Touramanis,³⁶ A. J. Bevan,³⁷ F. Di Lodovico,³⁷ R. Sacco,³⁷ M. Sigamani,³⁷ G. Cowan,³⁸ D. N. Brown,³⁹ C. L. Davis,³⁹ A. G. Denig,⁴⁰ M. Fritsch,⁴⁰ W. Gradl,⁴⁰ A. Hafner,⁴⁰ E. Prencipe,⁴⁰ D. Bailey,⁴¹ R. J. Barlow,^{41,‡} G. Jackson,⁴¹ G. D. Lafferty,⁴¹ E. Behn,⁴² R. Cenci,⁴² B. Hamilton,⁴² A. Jawahery,⁴² D. A. Roberts,⁴² G. Simi,⁴² C. Dallapiccola,⁴³ R. Cowan,⁴⁴ D. Dujmic,⁴⁴ G. Sciolla,⁴⁴ R. Cheaib,⁴⁵ D. Lindemann,⁴⁵ P. M. Patel,⁴⁵ S. H. Robertson,⁴⁵ M. Schram,⁴⁵ P. Biassoni,^{46a,46b} N. Neri,^{46a} F. Palombo,^{46a,46b} S. Stracka,^{46a,46b} L. Cremaldi,⁴⁷ R. Godang,^{47,§} R. Kroeger,⁴⁷ P. Sonnek,⁴⁷ D. J. Summers,⁴⁷ X. Nguyen,⁴⁸ M. Simard,⁴⁸ P. Taras,⁴⁸ G. De Nardo,^{49a,49b} D. Monorchio,^{49a,49b} G. Onorato,^{49a,49b} C. Sciacca,^{49a,49b} M. Martinelli,⁵⁰ G. Raven,⁵⁰ C. P. Jessop,⁵¹ K. J. Knoepfel,⁵¹ J. M. LoSecco,⁵¹ W. F. Wang,⁵¹ K. Honscheid,⁵² R. Kass,⁵² J. Brau,⁵³ R. Frey,⁵³ N. B. Sinev,⁵³ D. Strom,⁵³ E. Torrence,⁵³ E. Feltresi,^{54a,54b} N. Gagliardi,^{54a,54b} M. Margoni,^{54a,54b} M. Morandin,^{54a} M. Posocco,^{54a} M. Rotondo,^{54a} F. Simonetto,^{54a,54b} R. Stroili,^{54a,54b} S. Akar,⁵⁵ E. Ben-Haim,⁵⁵ M. Bomben,⁵⁵ G. R. Bonneaud,⁵⁵ H. Briand,⁵⁵ G. Calderini,⁵⁵ J. Chauveau,⁵⁵ O. Hamon,⁵⁵ Ph. Leruste,⁵⁵ G. Marchiori,⁵⁵ J. Ocariz,⁵⁵ S. Sitt,⁵⁵ M. Biasini,^{56a,56b} E. Manoni,^{56a,56b} S. Pacetti,^{56a,56b} A. Rossi,^{56a,56b} C. Angelini,^{57a,57b} G. Batignani,^{57a,57b} S. Bettarini,^{57a,57b} M. Carpinelli,^{57a,57b,||} G. Casarosa,^{57a,57b} A. Cervelli,^{57a,57b} F. Forti,^{57a,57b} M. A. Giorgi,^{57a,57b} A. Lusiani,^{57a,57c} B. Oberhof,^{57a,57b} E. Paoloni,^{57a,57b} A. Perez,^{57a} G. Rizzo,^{57a,57b} J. J. Walsh,^{57a} D. Lopes Pegna,⁵⁸ J. Olsen,⁵⁸ A. J. S. Smith,⁵⁸ A. V. Telnov,⁵⁸ F. Anulli,^{59a} G. Cavoto,^{59a} R. Faccini,^{59a,59b} F. Ferrarotto,^{59a} F. Ferroni,^{59a,59b} M. Gaspero,^{59a,59b} L. Li Gioi,^{59a} M. A. Mazzoni,^{59a} G. Piredda,^{59a} C. Büniger,⁶⁰ O. Grünberg,⁶⁰ T. Hartmann,⁶⁰ T. Leddig,⁶⁰ H. Schröder,⁶⁰ C. Voss,⁶⁰ R. Waldi,⁶⁰ T. Adye,⁶¹ E. O. Olaiya,⁶¹ F. F. Wilson,⁶¹ S. Emery,⁶² G. Hamel de Monchenault,⁶² G. Vasseur,⁶² Ch. Yèche,⁶² D. Aston,⁶³ D. J. Bard,⁶³ R. Bartoldus,⁶³ C. Cartaro,⁶³ M. R. Convery,⁶³ J. Dorfan,⁶³ G. P. Dubois-Felsmann,⁶³ W. Dunwoodie,⁶³ M. Ebert,⁶³ R. C. Field,⁶³ M. Franco Sevilla,⁶³ B. G. Fulson,⁶³ A. M. Gabareen,⁶³ M. T. Graham,⁶³ P. Grenier,⁶³ C. Hast,⁶³ W. R. Innes,⁶³ M. H. Kelsey,⁶³ P. Kim,⁶³ M. L. Kocian,⁶³ D. W. G. S. Leith,⁶³ P. Lewis,⁶³ B. Lindquist,⁶³ S. Luitz,⁶³ V. Luth,⁶³ H. L. Lynch,⁶³ D. B. MacFarlane,⁶³ D. R. Muller,⁶³ H. Neal,⁶³ S. Nelson,⁶³ M. Perl,⁶³ T. Pulliam,⁶³ B. N. Ratcliff,⁶³ A. Roodman,⁶³ A. A. Salnikov,⁶³ R. H. Schindler,⁶³ A. Snyder,⁶³ D. Su,⁶³ M. K. Sullivan,⁶³ J. Va'vra,⁶³ A. P. Wagner,⁶³ M. Weaver,⁶³ W. J. Wisniewski,⁶³ M. Wittgen,⁶³ D. H. Wright,⁶³ H. W. Wulsin,⁶³ C. C. Young,⁶³ V. Ziegler,⁶³ W. Park,⁶⁴ M. V. Purohit,⁶⁴ R. M. White,⁶⁴ J. R. Wilson,⁶⁴ A. Randle-Conde,⁶⁵ S. J. Sekula,⁶⁵ M. Bellis,⁶⁶ J. F. Benitez,⁶⁶ P. R. Burchat,⁶⁶ T. S. Miyashita,⁶⁶ M. S. Alam,⁶⁷ J. A. Ernst,⁶⁷ R. Gorodeisky,⁶⁸ N. Guttman,⁶⁸ D. R. Peimer,⁶⁸ A. Soffer,⁶⁸ P. Lund,⁶⁹ S. M. Spanier,⁶⁹ R. Eckmann,⁷⁰ J. L. Ritchie,⁷⁰ A. M. Ruland,⁷⁰ C. J. Schilling,⁷⁰ R. F. Schwitters,⁷⁰ B. C. Wray,⁷⁰ J. M. Izen,⁷¹ X. C. Lou,⁷¹ F. Bianchi,^{72a,72b} D. Gamba,^{72a,72b} L. Lanceri,^{73a,73b} L. Vitale,^{73a,73b} F. Martinez-Vidal,⁷⁴ A. Oyanguren,⁷⁴ H. Ahmed,⁷⁵ J. Albert,⁷⁵ Sw. Banerjee,⁷⁵ F. U. Bernlochner,⁷⁵ H. H. F. Choi,⁷⁵ G. J. King,⁷⁵ R. Kowalewski,⁷⁵ M. J. Lewczuk,⁷⁵

I. M. Nugent,⁷⁵ J. M. Roney,⁷⁵ R. J. Sobie,⁷⁵ N. Tasneem,⁷⁵ T. J. Gershon,⁷⁶ P. F. Harrison,⁷⁶ T. E. Latham,⁷⁶
E. M. T. Puccio,⁷⁶ H. R. Band,⁷⁷ S. Dasu,⁷⁷ Y. Pan,⁷⁷ R. Prepost,⁷⁷ and S. L. Wu⁷⁷

(BABAR Collaboration)

- ¹Laboratoire d'Annecy-le-Vieux de Physique des Particules (LAPP), Université de Savoie,
CNRS/IN2P3, F-74941 Annecy-Le-Vieux, France
- ²Universitat de Barcelona, Facultat de Física, Departament ECM, E-08028 Barcelona, Spain
- ^{3a}INFN Sezione di Bari, I-70126 Bari, Italy
- ^{3b}Dipartimento di Fisica, Università di Bari, I-70126 Bari, Italy
- ⁴Institute of Physics, University of Bergen, N-5007 Bergen, Norway
- ⁵Lawrence Berkeley National Laboratory and University of California, Berkeley, California 94720, USA
- ⁶Ruhr Universität Bochum, Institut für Experimentalphysik I, D-44780 Bochum, Germany
- ⁷University of British Columbia, Vancouver, British Columbia, Canada V6T 1Z1
- ⁸Brunel University, Uxbridge, Middlesex UB8 3PH, United Kingdom
- ⁹Budker Institute of Nuclear Physics, Novosibirsk 630090, Russia
- ¹⁰University of California at Irvine, Irvine, California 92697, USA
- ¹¹University of California at Riverside, Riverside, California 92521, USA
- ¹²University of California at Santa Barbara, Santa Barbara, California 93106, USA
- ¹³University of California at Santa Cruz, Institute for Particle Physics, Santa Cruz, California 95064, USA
- ¹⁴California Institute of Technology, Pasadena, California 91125, USA
- ¹⁵University of Cincinnati, Cincinnati, Ohio 45221, USA
- ¹⁶University of Colorado, Boulder, Colorado 80309, USA
- ¹⁷Colorado State University, Fort Collins, Colorado 80523, USA
- ¹⁸Technische Universität Dortmund, Fakultät Physik, D-44221 Dortmund, Germany
- ¹⁹Technische Universität Dresden, Institut für Kern- und Teilchenphysik, D-01062 Dresden, Germany
- ²⁰Laboratoire Leprince-Ringuet, Ecole Polytechnique, CNRS/IN2P3, F-91128 Palaiseau, France
- ²¹University of Edinburgh, Edinburgh EH9 3JZ, United Kingdom
- ^{22a}INFN Sezione di Ferrara, I-44100 Ferrara, Italy
- ^{22b}Dipartimento di Fisica, Università di Ferrara, I-44100 Ferrara, Italy
- ²³INFN Laboratori Nazionali di Frascati, I-00044 Frascati, Italy
- ^{24a}INFN Sezione di Genova, I-16146 Genova, Italy
- ^{24b}Dipartimento di Fisica, Università di Genova, I-16146 Genova, Italy
- ²⁵Indian Institute of Technology Guwahati, Guwahati, Assam, 781 039, India
- ²⁶Harvard University, Cambridge, Massachusetts 02138, USA
- ²⁷Harvey Mudd College, Claremont, California 91711
- ²⁸Physikalisches Institut, Universität Heidelberg, Philosophenweg 12, D-69120 Heidelberg, Germany
- ²⁹Humboldt-Universität zu Berlin, Institut für Physik, Newtonstr. 15, D-12489 Berlin, Germany
- ³⁰Imperial College London, London, SW7 2AZ, United Kingdom
- ³¹University of Iowa, Iowa City, Iowa 52242, USA
- ³²Iowa State University, Ames, Iowa 50011-3160, USA
- ³³Johns Hopkins University, Baltimore, Maryland 21218, USA
- ¹Laboratoire de l'Accélérateur Linéaire, IN2P3/CNRS et Université Paris-Sud 11,
Centre Scientifique d'Orsay, B. P. 34, F-91898 Orsay Cedex, France
- ³⁵Lawrence Livermore National Laboratory, Livermore, California 94550, USA
- ³⁶University of Liverpool, Liverpool L69 7ZE, United Kingdom
- ³⁷Queen Mary, University of London, London, E1 4NS, United Kingdom
- ³⁸University of London, Royal Holloway and Bedford New College, Egham, Surrey TW20 0EX, United Kingdom
- ³⁹University of Louisville, Louisville, Kentucky 40292, USA
- ⁴⁰Johannes Gutenberg-Universität Mainz, Institut für Kernphysik, D-55099 Mainz, Germany
- ⁴¹University of Manchester, Manchester M13 9PL, United Kingdom
- ⁴²University of Maryland, College Park, Maryland 20742, USA
- ⁴³University of Massachusetts, Amherst, Massachusetts 01003, USA
- ⁴⁴Massachusetts Institute of Technology, Laboratory for Nuclear Science, Cambridge, Massachusetts 02139, USA
- ⁴⁵McGill University, Montréal, Québec, Canada H3A 2T8
- ^{46a}INFN Sezione di Milano, I-20133 Milano, Italy
- ^{46b}Dipartimento di Fisica, Università di Milano, I-20133 Milano, Italy
- ⁴⁷University of Mississippi, University, Mississippi 38677, USA
- ⁴⁸Université de Montréal, Physique des Particules, Montréal, Québec, Canada H3C 3J7
- ^{49a}INFN Sezione di Napoli, I-80126 Napoli, Italy

^{49b}*Dipartimento di Scienze Fisiche, Università di Napoli Federico II, I-80126 Napoli, Italy*

⁵⁰*NIKHEF, National Institute for Nuclear Physics and High Energy Physics, NL-1009 DB Amsterdam, The Netherlands*

⁵¹*University of Notre Dame, Notre Dame, Indiana 46556, USA*

⁵²*Ohio State University, Columbus, Ohio 43210, USA*

⁵³*University of Oregon, Eugene, Oregon 97403, USA*

^{54a}*INFN Sezione di Padova, I-35131 Padova, Italy*

^{54b}*Dipartimento di Fisica, Università di Padova, I-35131 Padova, Italy*

⁵⁵*Laboratoire de Physique Nucléaire et de Hautes Energies, IN2P3/CNRS, Université Pierre et Marie Curie-Paris6,*

Université Denis Diderot-Paris7, F-75252 Paris, France

^{56a}*INFN Sezione di Perugia, I-06100 Perugia, Italy*

^{56b}*Dipartimento di Fisica, Università di Perugia, I-06100 Perugia, Italy*

^{57a}*INFN Sezione di Pisa, I-56127 Pisa, Italy*

^{57b}*Dipartimento di Fisica, Università di Pisa, I-56127 Pisa, Italy*

^{57c}*Scuola Normale Superiore di Pisa, I-56127 Pisa, Italy*

⁵⁸*Princeton University, Princeton, New Jersey 08544, USA*

^{59a}*INFN Sezione di Roma, I-00185 Roma, Italy*

^{59b}*Dipartimento di Fisica, Università di Roma La Sapienza, I-00185 Roma, Italy*

⁶⁰*Universität Rostock, D-18051 Rostock, Germany*

⁶¹*Rutherford Appleton Laboratory, Chilton, Didcot, Oxon, OX11 0QX, United Kingdom*

⁶²*CEA, Irfu, SPP, Centre de Saclay, F-91191 Gif-sur-Yvette, France*

⁶³*SLAC National Accelerator Laboratory, Stanford, California 94309 USA*

⁶⁴*University of South Carolina, Columbia, South Carolina 29208, USA*

⁶⁵*Southern Methodist University, Dallas, Texas 75275, USA*

⁶⁶*Stanford University, Stanford, California 94305-4060, USA*

⁶⁷*State University of New York, Albany, New York 12222, USA*

⁶⁸*School of Physics and Astronomy, Tel Aviv University, Tel Aviv, 69978, Israel*

⁶⁹*University of Tennessee, Knoxville, Tennessee 37996, USA*

⁷⁰*University of Texas at Austin, Austin, Texas 78712, USA*

⁷¹*University of Texas at Dallas, Richardson, Texas 75083, USA*

^{72a}*INFN Sezione di Torino, I-10125 Torino, Italy*

^{72b}*Dipartimento di Fisica Sperimentale, Università di Torino, I-10125 Torino, Italy*

^{73a}*INFN Sezione di Trieste, I-34127 Trieste, Italy*

^{73b}*Dipartimento di Fisica, Università di Trieste, I-34127 Trieste, Italy*

⁷⁴*IFIC, Universitat de Valencia-CSIC, E-46071 Valencia, Spain*

⁷⁵*University of Victoria, Victoria, British Columbia, Canada V8W 3P6*

⁷⁶*Department of Physics, University of Warwick, Coventry CV4 7AL, United Kingdom*

⁷⁷*University of Wisconsin, Madison, Wisconsin 53706, USA*

(Received 8 February 2012; published 21 May 2012)

Recent astrophysical and terrestrial experiments have motivated the proposal of a dark sector with GeV-scale gauge boson force carriers and new Higgs bosons. We present a search for a dark Higgs boson using 516 fb^{-1} of data collected with the *BABAR* detector. We do not observe a significant signal and we set 90% confidence level upper limits on the product of the standard model-dark-sector mixing angle and the dark-sector coupling constant.

DOI: 10.1103/PhysRevLett.108.211801

PACS numbers: 14.80.Ec, 12.60.-i, 95.35.+d

While the astrophysical evidence for dark matter is now overwhelming, its precise nature and origin remain elusive. Recent results from terrestrial and satellite experiments have motivated the proposal of a new, hidden gauge sector under which WIMP-like dark matter particles are charged [1–3]. An Abelian gauge field, the dark photon A' , couples this dark sector to standard model (SM) particles through its kinetic mixing with the SM hypercharge fields [4]. In this framework dark matter particles can annihilate into pairs of dark photons, which subsequently decay to SM particles. The dark photon mass is constrained to be at most a few GeV to be compatible with astrophysical constraints

[5,6]. In a minimal model [7], the dark photon mass is generated via the Higgs mechanism, adding a dark Higgs boson h' to the theory. The mass hierarchy between these two particles is not constrained, and the dark Higgs boson could be light as well.

A consequence of this scenario is the possibility of probing a light dark sector at low-energy e^+e^- colliders [7,8] and fixed-target experiments [9,10]. Searches for dark photon production have yielded negative results, and constraints have been derived on the mixing strength between the SM and the dark sector, ϵ , as a function of the dark photon mass [9].

The Higgs-strahlung process, $e^+e^- \rightarrow A'h', h' \rightarrow A'A'$, might offer another gateway to a dark sector. This reaction is of particular interest, since it is one of the few process suppressed by a single factor of ϵ , and the background is expected to be small. If observed, this reaction could provide an unambiguous signature of physics beyond the standard model. The event topology depends on the dark Higgs boson and dark photon masses. While Higgs bosons heavier than two dark photons decay promptly, their lifetime becomes large enough to escape undetected for $m_{h'} < m_{A'}$. Moreover, the dark photon width is proportional to $m_{A'}\epsilon^2$, and its decay can be prompt or displaced, depending on the value of these parameters. At *BABAR* energies, the decay length in the detector is $\mathcal{O}(100)$ μm or less for $m_{A'} > 250$ MeV and $\epsilon \gtrsim 10^{-4}$, and dark photon decays can be considered as prompt in this regime.

We report a search for dark Higgs production in the Higgs-strahlung process. The measurement is performed in the range $0.8 < m_{h'} < 10.0$ GeV and $0.25 < m_{A'} < 3.0$ GeV with the constraint $m_{h'} > 2m_{A'}$. To avoid any experimental bias, the data are not examined before the selection procedure is finalized. The data sample used in this analysis consists of 521 fb^{-1} of data collected mostly at the $Y(4S)$ resonance, but also including luminosity at the $Y(3S)$ and $Y(2S)$ peaks, as well as off-resonance data. A sample corresponding to $\sim 10\%$ of the data (optimization sample) is used to optimize the selection criteria and is discarded from the final data set. This sample is treated entirely as background for optimization and background studies.

The *BABAR* detector is described in detail elsewhere [11]. Charged-particle momenta are measured in a tracking system formed by a five-layer double-sided silicon vertex detector and a 40-layer central drift chamber both immersed in a 1.5 T axial magnetic field. Electron and photon energies are measured in a CsI(Tl) electromagnetic calorimeter. Charged-particle identification (PID) is performed using an internally reflecting ring-imaging Cherenkov detector and the energy loss dE/dx measured by the silicon vertex detector and central drift chamber. Muons are mainly identified by the instrumented magnetic flux return.

Signal events are generated by MADGRAPH [12] for about 40 different hypotheses of dark photon and Higgs boson masses. The hadronization of the $A' \rightarrow q\bar{q}$ ($q = u, d, s, c$) decay is performed by JETSET [13]. The detector acceptance is studied using Monte Carlo (MC) simulation based on GEANT4 [14]. Time-dependent detector inefficiencies, as monitored during data taking periods, are included in the simulation.

The $e^+e^- \rightarrow A'h', h' \rightarrow A'A'$ reaction is either fully reconstructed in the $3(l^+l^-)$, $2(l^+l^-)\pi^+\pi^-$ and $l^+l^-2(\pi^+\pi^-)$ final states ($l = e, \mu$), or partially reconstructed in the $2(\mu^+\mu^-) + X$ and $\mu^+\mu^-e^+e^- + X$ channels, where X denotes any final state other than a pair of pions or leptons. The $2(e^+e^-) + X$ mode suffers from

significantly more background than the other channels and is excluded. The first modes are collectively referred to as “exclusive modes”, as opposed to “inclusive modes” for the $2(l^+l^-) + X$ channels. The inclusive modes are only considered in the region $m_{A'} > 1.2$ GeV, since their contribution is small below this threshold and the background level becomes large.

The event selection proceeds by first reconstructing dark photon candidates from pairs of oppositely-charged tracks identified as electrons, muons or pions by PID algorithms. In addition, the helicity angle of the electron in the dark photon rest frame, α_e , must satisfy $\cos\alpha_e < 0.9$. The background from accidental e^+e^- pairs exhibits a peaking component near $\cos\alpha_e \sim 1$, while signal events are broadly distributed. Events are then processed according to the following sequence of hypotheses until a match is found: 6μ , $4\mu 2e$, $2\mu 4e$, $6e$, $4\mu 2\pi$, $2\mu 2e 2\pi$, $4e 2\pi$, $2\mu 4\pi$, $2e 4\pi$, $4\mu + X$, $2\mu 2e + X$. This order is chosen to minimize the cross-feed between channels and the efficiency loss due to misclassification.

Additional criteria are applied to increase the purity of the signal. Exclusive modes must contain exactly six charged tracks, and the invariant mass of the three dark photon system must be larger than 95% of the e^+e^- center-of-mass energy. The dark photons are then fitted, constraining the tracks to originate from the interaction point. The fit probability is required to be larger than 10^{-5} . Finally, the largest mass difference between the dark photon candidates, ΔM , must be less than 10–240 MeV, depending on the final state and the dark photon masses. The distribution of this variable after all other selection criteria are applied is displayed in Fig. 1 for the $2e 4\pi$ final state. The signal peaks near $\Delta M \sim 0$, while the background is concentrated towards higher values.

Inclusive modes are selected by requiring two leptonic dark photon candidates with similar masses. The two dark photons are fitted, constraining the four leptons to originate from the interaction point. Events with a fit probability less than 10^{-5} are discarded. The remaining dark photon is then identified as the system recoiling against the two lepton pairs. The cosine of its polar angle in the laboratory frame must be less than 0.99 to remove radiative QED events. Finally, the masses of all dark photons must be compatible within their uncertainties.

A total of six events are selected by these criteria: one $4\mu 2\pi$, two $2\mu 4\pi$, two $2e 4\pi$ and one $4\mu + X$ events. No candidate containing six leptons survives the selection. The distribution of the dark photon mass versus the dark Higgs boson mass is shown in Fig. 2. Three entries, corresponding to the possible assignments of the decay $h' \rightarrow A'A'$, are considered for each event. Besides the contribution of $\rho \rightarrow \pi^+\pi^-$ or $\omega \rightarrow \pi^+\pi^-$ decays near $m_{A'} \sim 0.7\text{--}0.8$ GeV, no significant signal is observed. This result is consistent with the two events observed in the optimization sample, assumed to be background. Given these limited

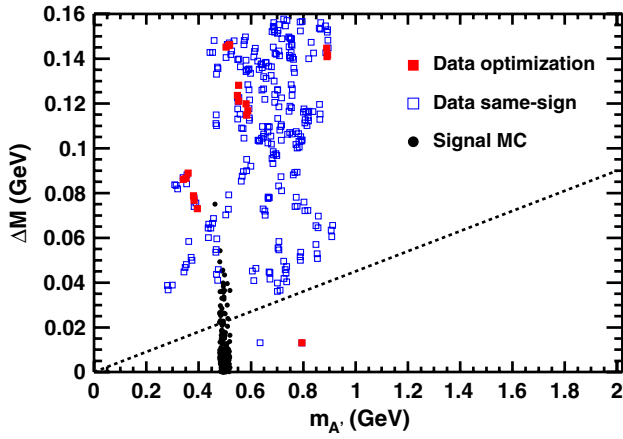


FIG. 1 (color online). Distribution of the largest mass difference between the three dark photon candidates (ΔM) versus the average dark photon mass ($m_{A'}$) after all other selection criteria are applied for the $2e4\pi$ final state. The data are shown for opposite-sign combinations from the optimization sample (plain squares) as well as an additional background estimation, described later, of same-sign combinations from the full data set (open squares). The Monte Carlo predictions for $m_{h'} = 3.0$ GeV and $m_{A'} = 0.5$ GeV are displayed as plain circles. The signal region for the $2e4\pi$ mode is delimited by the dashed line.

statistics, a second background estimation based on the full data set using same-sign combinations, such as $(e^+e^-(\mu^+\mu^+)(\mu^-\mu^-)$ or $(e^+e^+)(\mu^-\mu^-)X$, is used as a cross-check. Both methods predict background levels consistent within their statistical uncertainties.

Using uniform priors in the cross-section, 90% confidence level (CL) Bayesian upper limits on the production cross-section are derived for each mode separately as a function of the dark Higgs and dark photon masses. The $(m_{h'}, m_{A'})$ plane is scanned in steps of 10 MeV in both directions between $0.8 < m_{h'} < 10$ GeV and $0.25 < m_{A'} < 3$ GeV. For each mass hypothesis, the signal region

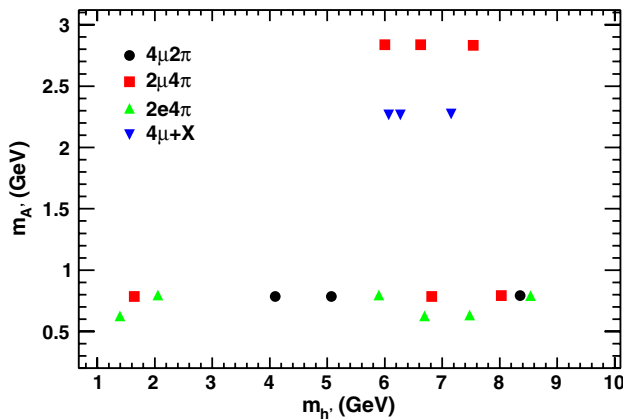


FIG. 2 (color online). Distribution of dark photon mass ($m_{A'}$) versus the dark Higgs mass ($m_{h'}$) for the final data sample. Three entries are plotted for each event, corresponding to the possible assignments of the decay $h' \rightarrow A'A'$.

is taken as the interval $m_{h'} - 5\sigma_{m_{h'}} < m_{h'} < m_{h'} + 3\sigma_{m_{h'}}$ and $m_{A'} - 5\sigma_{m_{A'}} < m_{A'} < m_{A'} + 3\sigma_{m_{A'}}$, where $\sigma_{m_{A'}}$ ($\sigma_{m_{h'}}$) denotes the corresponding dark photon (Higgs) mass resolution. An asymmetric range is used to accommodate the non-Gaussian tail of the low-mass side of the signal. The dark photon (Higgs) mass resolution varies between 2–17 MeV (3–55 MeV), depending on the dark photon (Higgs) mass and final state. While setting the limits we adopt the most conservative approach, treating as signal every observed event in the signal region. The systematic uncertainties are included by convolving the likelihood of each final state with Gaussian distributions having variances equal to the systematic uncertainties described below taking correlations into account.

The efficiency is determined for several values of dark photon and Higgs boson masses, and is linearly interpolated between the known points. The efficiency includes acceptance, trigger, selection criteria and the dark photon branching fraction. The branching fractions into leptons and hadrons are given by $BF(A' \rightarrow \ell^+\ell^-) = 1/(2+R)$, $BF(A' \rightarrow \text{hadrons}) = R/(2+R)$ and $BF(A' \rightarrow \pi^+\pi^-) = BF(A' \rightarrow \text{hadrons})\sigma(e^+e^- \rightarrow \pi^+\pi^-)/\sigma(e^+e^- \rightarrow \text{hadrons})$, where R denotes the ratio $\sigma(e^+e^- \rightarrow \text{hadrons})/\sigma(e^+e^- \rightarrow \mu^+\mu^-)$ [15]. The efficiency increases from a few per mille in regions with small branching fractions to 33% for the six electron mode in the region $m_{A'} < 0.2$ GeV. It drops rapidly in the region $m_{h'} < 0.8$ GeV and $m_{h'} > 10$ GeV, as tracks produced by dark photon decays have a low transverse momentum or are emitted close to the beam and are not reconstructed.

The limits on each channel are then combined to extract 90% CL upper limits on the $e^+e^- \rightarrow A'h', h' \rightarrow A'A'$ cross

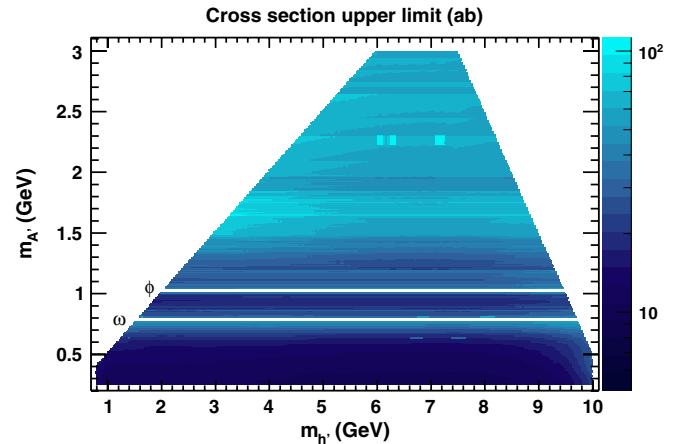


FIG. 3 (color online). Upper limit (90% CL) on the $e^+e^- \rightarrow A'h', h' \rightarrow A'A'$ cross-section as a function of the dark photon and dark Higgs masses. The limits in the ω - and ϕ -meson regions are orders of magnitude larger than the average limits and the corresponding regions (horizontal bands centered around $m_{A'} \sim 0.78$ GeV and $m_{A'} \sim 1.04$ GeV) are masked to avoid overflow.

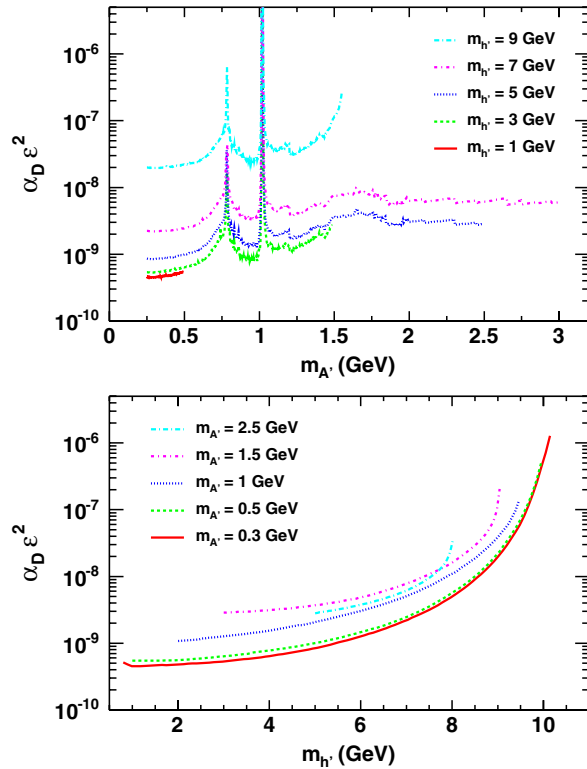


FIG. 4 (color online). Upper limit (90% CL) on the product $\alpha_D \epsilon^2$ as a function of the dark photon mass for selected values of dark Higgs boson masses (top) and as a function of the dark Higgs boson mass for selected values of dark photon masses (bottom).

section. The results are displayed in Fig. 3. The limits are typically at the level of 10–100 ab.

The major contribution to the systematic uncertainty arises from the extrapolation procedure used to determine the efficiency, which is estimated by comparing the extrapolated value to the nearest known point. This uncertainty increases from 1% to 8% in some corners of the phase space. The uncertainty on the branching fractions ranges from a few per mille to 4%. The uncertainty due to the modeling of $A' \rightarrow$ hadron decays in inclusive modes is estimated by comparing different fragmentation models. This systematic is found to be 4% reflecting the limited sensitivity of the selection procedure to the hadronic system produced by the dark photon decay. The uncertainty due to PID algorithms varies between 1.5% and 4.5%, assessed using high-purity samples of leptons and pions. Additional uncertainties include the determination of the track reconstruction efficiency (1.2%), luminosity (0.6%), and the limited Monte Carlo statistics (0.5%–2.4%).

The limits on the $e^+e^- \rightarrow A'h'$, $h' \rightarrow A'A'$ cross section are finally translated into 90% CL upper limits on the product $\alpha_D \epsilon^2$, where $\alpha_D = g_D^2/4\pi$ and g_D is the dark-sector gauge coupling [7]. The results are displayed in Fig. 4 as a function of the dark photon (Higgs) mass for selected values of the dark Higgs boson (photon) mass.

Values down to 10^{-10} – 10^{-8} are excluded for a large range of dark photon and dark Higgs masses. These results assume prompt dark Higgs boson and dark photon decays.

In conclusion, a search for dark Higgs boson production has been performed in the range $0.25 < m_{A'} < 3$ GeV and $0.8 < m_{h'} < 10$ GeV for $m_{h'} > 2m_{A'}$. No signal has been observed and upper limits on the product of the mixing angle and the dark coupling constant in the case of a hidden sector with an Abelian Higgs boson have been set at the level of 10^{-10} – 10^{-8} . Assuming $\alpha_D = \alpha$, these measurements translate into limits on the mixing strength in the range 10^{-4} – 10^{-3} , an order of magnitude smaller than the current bounds.

The authors wish to thank R. Essig, N. Toro, and P. Schuster for useful discussions on theoretical issues. We are grateful for the excellent luminosity and machine conditions provided by our PEP-II colleagues, and for the substantial dedicated effort from the computing organizations that support *BABAR*. The collaborating institutions wish to thank SLAC for its support and kind hospitality. This work is supported by DOE and NSF (USA), NSERC (Canada), CEA and CNRS-IN2P3 (France), BMBF and DFG (Germany), INFN (Italy), FOM (The Netherlands), NFR (Norway), MES (Russia), MICIIN (Spain), STFC (United Kingdom). Individuals have received support from the Marie Curie EIF (European Union), the A.P. Sloan Foundation (USA) and the Binational Science Foundation (USA-Israel).

*Present address: The University of Tabuk, Tabuk 71491, Saudi Arabia.

†Also with Università di Perugia, Dipartimento di Fisica, Perugia, Italy.

‡Present address: The University of Huddersfield, Huddersfield HD1 3DH, UK.

§Present address: University of South Alabama, Mobile, AL 36688, USA.

||Also with Università di Sassari, Sassari, Italy.

- [1] P. Fayet, *Phys. Rev. D* **75**, 115017 (2007).
- [2] M. Pospelov, A. Ritz, and M. B. Voloshin, *Phys. Lett. B* **662**, 53 (2008).
- [3] N. Arkani-Hamed, D. P. Finkbeiner, T. R. Slatyer, and N. Weiner, *Phys. Rev. D* **79**, 015014 (2009).
- [4] B. Holdom, *Phys. Lett. B* **166**, 196 (1986).
- [5] O. Adriani *et al.* (PAMELA Collaboration), *Nature (London)* **458**, 607 (2009).
- [6] M. Ackermann *et al.* (Fermi LAT Collaboration), *Phys. Rev. D* **82**, 092004 (2010).
- [7] B. Batell, M. Pospelov, and A. Ritz, *Phys. Rev. D* **79**, 115008 (2009).
- [8] R. Essig, P. Schuster, and N. Toro, *Phys. Rev. D* **80**, 015003 (2009) and references therein.
- [9] J. D. Bjorken, R. Essig, P. Schuster, and N. Toro, *Phys. Rev. D* **80**, 075018 (2009).
- [10] B. Batell, M. Pospelov, and A. Ritz, *Phys. Rev. D* **80**, 095024 (2009).

-
- [11] B. Aubert *et al.* (BABAR Collaboration), *Nucl. Instrum. Methods Phys. Res., Sect. A* **479**, 1 (2002).
- [12] J. Alwall, P. Demin, S. de Visscher, R. Frederix, M. Herquet, F. Maltoni, T. Plehn, and D.L. Rainwater *et al.*, *J. High Energy Phys.* **09** (2007) 028.
- [13] T. Sjostrand, *Comput. Phys. Commun.* **82**, 74 (1994).
- [14] S. Agostinelli *et al.* (GEANT4 Collaboration), *Nucl. Instrum. Methods Phys. Res., Sect. A* **506**, 250 (2003).
- [15] K. Nakamura *et al.* (Particle Data Group), *J. Phys. G* **37**, 075021 (2010) and 2011 partial update for the 2012 edition.